Original Article

Correlation between apparent diffusion coefficient and tumor-stroma ratio in hybrid ^{18}F-FDG PET/MRI: preliminary results of a rectal cancer cohort study

Shidong Hu[1#], Xiaowei Xing[2#], Jiajin Liu[3#], Xi Liu[4], Jinhang Li[5], Wei Jin[5], Songyan Li[1], Yang Yan[1], Da Teng[1], Boyan Liu[1], Yufeng Wang[6], Baixuan Xu[3*], Xiaohui Du[1*]

[1]Department of General Surgery, The First Medical Center, Chinese People's Liberation Army (PLA) General Hospital, Beijing, China; [2]Department of Hernia and Abdominal Wall Surgery, Beijing Chaoyang Hospital, Capital Medical University, Beijing, China; [3]Department of Nuclear Medicine, The First Medical Center, Chinese People's Liberation Army (PLA) General Hospital, Beijing, China; [4]Key Laboratory of Carcinogenesis and Translational Research (Ministry of Education), Department of Radiology, Peking University Cancer Hospital and Institute, Beijing, China; [5]Department of Pathology, The First Medical Center, Chinese People's Liberation Army (PLA) General Hospital, Beijing, China; [6]Department of Hospital Management, The First Medical Center, Chinese People's Liberation Army (PLA) General Hospital, Beijing, China

Contributions: (I) Conception and design: X Du, B Xu, S Hu, X Xing; (II) Administrative support: X Du, B Xu; (III) Provision of study materials or patients: X Xing, J Liu, S Li, Y Yan, D Teng, B Liu, Y Wang; (IV) Collection and assembly of data: S Hu, X Xing, J Liu, X Liu, J Li, W Jin; (V) Data analysis and interpretation: S Hu, J Liu, X Liu; (VI) Manuscript writing: All authors; (VII) Final approval of manuscript: All authors.

[#]These authors contributed equally to this work.

[*]These authors contributed equally to this work.

Correspondence to: Xiaohui Du. Department of General Surgery, The First Medical Center, Chinese People's Liberation Army (PLA) General Hospital, Beijing 100853, China. Email: duxiaohui301pw@163.com; Baixuan Xu. Department of Nuclear Medicine, The First Medical Center, Chinese People's Liberation Army (PLA) General Hospital, Beijing 100853, China. Email: xubx301@163.com.

Background: To explore possible correlations between the tumor-stroma ratio (TSR) and different imaging features of fluorine-18-fluorodeoxyglucose positron emission tomography/magnetic resonance imaging (^{18}F-FDG PET/MRI) in untreated rectal cancer patients.

Methods: A patients with rectal cancer were included in this study. All participants were examined preoperatively with whole-body ^{18}F-FDG PET/MRI. Two pathologists evaluated the TSR of tumors together. Apparent diffusion coefficient (ADC) values and PET-related parameters of the primary lesions were measured and compared between the stroma-high and stroma-low groups. Pearson's correlation or Spearman's rank correlation were used to evaluate the correlation between the ADC values, PET-related parameters, and pathological indices.

Results: Our results showed that in the untreated rectal cancer patients, the ADC mean values correlated with the TSR (r=0.327; P=0.007), and stroma-high (low TSR) rectal cancer corresponded to relatively lower ADC mean values (813.54±88.68 *vs.* 879.92±133.18; P=0.018). The ADC mean and ADC minimum (ADCmin) values were found to be negatively correlated with the pathological T stages (r=–0.384, P=0.001; r=–0.416, P=0.001, respectively) as well as the largest tumor diameters (r=–0.340, P=0.005; r=–0.314, P=0.010, respectively) of rectal cancer. In addition, the pathological T stages correlated with all PET-related metabolic parameters, including mean standard uptake value (SUV), maximum SUV (SUVmax), metabolic tumor volume (MTV), and total lesion glycolysis (TLG) (r=0.338, P=0.006; r=0.350, P=0.004; r=0.326, P=0.007; and r=0.472, P<0.001, respectively). Our results also identified associations between the ADCmin values and SUVmean, SUVmax, and TLG (r=–0.335, P=0.006; r=–0.343, P=0.005; and r=–0.343, P=0.005, respectively). However, there were no statistical correlations between the PET/MRI parameters and the

immunohistochemical (IHC) results.

Conclusions: This study indicated that the intratumoral heterogeneity measured by PET/MRI may reflect characteristics of the tumor microenvironment. Hence, PET/MRI parameters might be helpful in predicting tumor aggressiveness and prognosis.

Keywords: Rectal cancer; positron emission tomography/magnetic resonance imaging (PET/MRI); apparent diffusion coefficient (ADC); tumor-stroma ratio (TSR)

Submitted Sep 21, 2021. Accepted for publication May 17, 2022.
doi: 10.21037/qims-21-938
View this article at: https://dx.doi.org/10.21037/qims-21-938

Introduction

Colorectal cancer (CRC) is the third most frequently-occurring cancer and the second most common cause of cancer-related deaths worldwide, and rectal cancer accounts for 30–40% of CRC (1). The mortality of CRC has decreased significantly due to the incredible improvements in treatment and diagnostic techniques (1). However, rectal cancer has a less favorable prognosis due to the high frequency of metastases and local recurrence (2). In rectal cancer, therapeutic decision making is primarily based on clinical tumor-node-metastasis (TNM) staging and pathological TNM staging can do is to judgment prognosis as well as to determine whether or not to administer adjuvant chemotherapy. Although the TNM staging system is still considered the most important factor in estimating patient prognosis (3), it seems insufficient for assessing the metastatic potential of rectal cancer, especially for patients with TNM stage II, which comprises heterogeneous subgroups with potentially different outcomes (4,5). Thus, there is a need for additional prognostic factors.

Tumor invasion and metastasis is considered a multifactorial process (6). The tumor microenvironment is composed of tumor cells and stroma, and the bidirectional communication between tumor cells and stroma plays an essential role in tumor growth, metabolism, and progression (7). Several studies have investigated the microenvironment of tumor cells by evaluating the tumor-stroma ratio (TSR), which has an important role in tumor cell invasion and metastasis (8-10). The TSR represents the relative amounts of tumor and intratumoral stroma, and generally, a high content of intratumoral stroma is associated with a poor prognosis (11). Intratumoral stroma and consensus molecular subtypes can be determined with pretreatment biopsy. However, preoperative biopsy samples are relatively superficial and sometimes fail to reflect the exact characteristics of the tumor.

Diffusion-weighted imaging (DWI) represents functional magnetic resonance (MR) techniques that can reflect internal alteration of the microenvironment and cellular density in tissues, and it has been applied in numerous cancers (12,13). Apparent diffusion coefficient (ADC) values derived from DWI are quantified and, more recently, have been considered a potential imaging parameter of tumor aggressiveness in rectal cancer (14,15). Previous studies have shown that the intensity of fluorine-18-fluorodeoxyglucose (^{18}F-FDG) uptake by malignant tumors is correlated with more aggressive tumor behavior, and high ^{18}F-FDG uptake in the primary tumor indicates a less favorable outcome (16-18). Recently, positron emission tomography/magnetic resonance imaging (PET/MRI) has emerged as a novel imaging technology that combines the metabolic information of PET and the anatomic and functional information of MRI in a single examination. We speculated whether histopathological features, including the TSR, influence ADC values and PET-related parameters in rectal cancer. Therefore, the purpose of this study was to explore possible correlations between the TSR and the different imaging parameters of ^{18}F-FDG PET/MRI in untreated rectal cancer. We present the following article in accordance with the STROBE reporting checklist (available at https://qims.amegroups.com/article/view/10.21037/qims-21-938/rc).

Methods

Patients

The study was conducted in accordance with the Declaration of Helsinki (as revised in 2013). The study was approved by the Institutional Review Board of The First Medical Center of the Chinese People's Liberation Army (PLA) General Hospital (No. S2017-083-01),

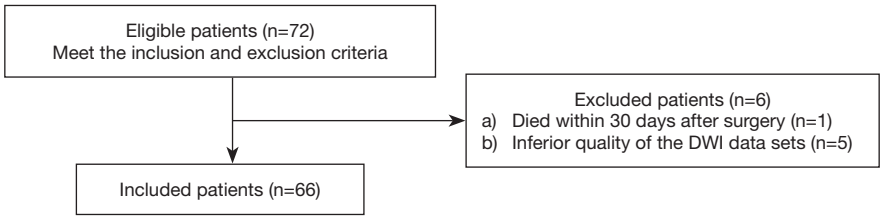

Figure 1 Flowchart of patient selection. DWI, diffusion-weighted imaging.

and informed consent was provided by all participants. In this cohort study, we prospectively enrolled patients with pathologically confirmed, primary rectal cancer at The First Medical Center of the Chinese PLA General Hospital from December 2016 to March 2019 (*Figure 1*). The inclusion criteria were as follows: (I) rectal cancer pathologically confirmed by enteroscopic biopsy; (II) prior total mesorectal excision (TME) surgery and pathological examination of resected tissue; (III) no contraindications to PET-MRI examination and no internal metal implants; and (IV) full disclosure of the research plan, and provision of signed informed consent. The exclusion criteria were as follows: (I) intolerance of general anesthesia or severe heart, lung, liver, and other major organ dysfunction; (II) severe coagulation disorder; (III) pregnancy; (IV) abdominal cavity or pelvic metastasis; (V) tumor perforation or acute peritonitis; or (VI) preoperative chemotherapy or radiation therapy. All participants were examined preoperatively with whole-body ^{18}F-FDG PET/MRI. Rectal cancer surgeries were performed according to TME principles.

PET/MRI protocol

All participants were examined in the supine position with a hybrid PET/MRI (Biograph mMR; Siemens Healthcare, Erlangen, Germany) scanner consisting of a 3-Tesla MRI scanner and an inline PET system equipped with an 8-channel phased array body coil. Participants fasted for at least 6 h before the PET/MRI examination to ensure a blood glucose level of <200 mg/dL. Scanning was performed 60 min after FDG injection and extended from the mid-thigh to the vertex of the scalp for a duration of approximately 50 min. Participants were informed to receive no bowel preparation before the examination, and no spasmolytic agent was used in this study. The MRI protocol consisted of a standard T2-weighted fast spin-echo sequence [repetition time/echo time (TR/TE): 4,300/78 ms, flip angle: 150°, slice thickness: 3 mm, intersection gap: 0.6 mm, field of view (FOV): 240×240 mm, matrix size: 320×310, acquisition time: 2 min 28 s] in 3 orthogonal directions and an axial DWI single-shot echo-planar sequence (TR/TE: 9,715/72 ms, slice thickness: 3 mm, intersection gap: 0.6 mm, FOV: 360×216 mm, matrix size: 110×110, acquisition time: 3 min 24 s), including b-values, b =50 and b =800 s/mm^2. The ADC maps were generated automatically by fitting a mono-exponential decay function to the b =50 and b =800 s/mm^2 images.

Image analysis

All PET/MRI data sets were independently reviewed and analyzed on a workstation (Syngo.Via; Siemens Healthcare) by a radiologist (XL, with 6 years of experience in interpreting MRI) and a nuclear medicine physician (JJL, with 8 years of experience in interpreting hybrid PET/MRI), who were blinded to each other's results and histopathological outcomes. The radiologist measured the parameters twice with a more than 2-week interval, and the nuclear medicine physician reanalyzed the measurements.

The contouring margins of tumor lesions were automatically derived and manually adjusted on axial, coronal, and sagittal planes in PET images to ensure accurate inclusion of the primary tumor while excluding adjacent normal structures, especially the hypermetabolic bladder (*Figure 2*). The values of the mean and maximum standard uptake value (SUVmean and SUVmax) were automatically measured. The metabolic tumor volume (MTV) was defined as the hypermetabolic tissue volume with a threshold of 42% of the SUVmax (19). The total lesion glycolysis (TLG) was calculated according to the formula: TLG = SUVmean × MTV (20). For the ADC measurement, the region of interest (ROI) was drawn manually along the edge of the largest tumor area section on the DWI image with a b-value of 800 s/mm^2. In addition, T2-weighted MRI and PET images were used as references to determine the border of the lesion on the corresponding section. Then, the ROI were copied to the corresponding ADC map (*Figure 3*). The values of mean

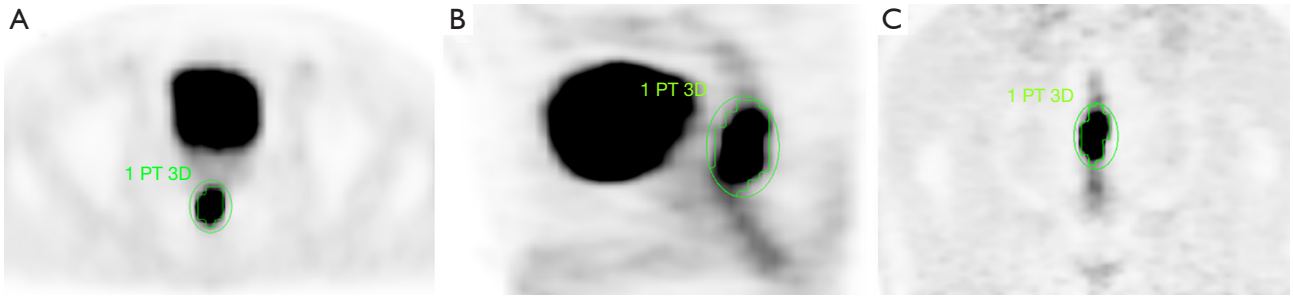

Figure 2 The contouring margins of the tumor lesion were automatically derived and manually adjusted on axial (A), sagittal (B), and coronal (C) planes in the ^{18}F-FDG PET/MRI image to ensure accurate inclusion of the primary tumor. PT, positron emission tomography; ^{18}F-FDG PET/MRI, fluorine-18-fluorodeoxyglucose-positron emission tomography/magnetic resonance imaging.

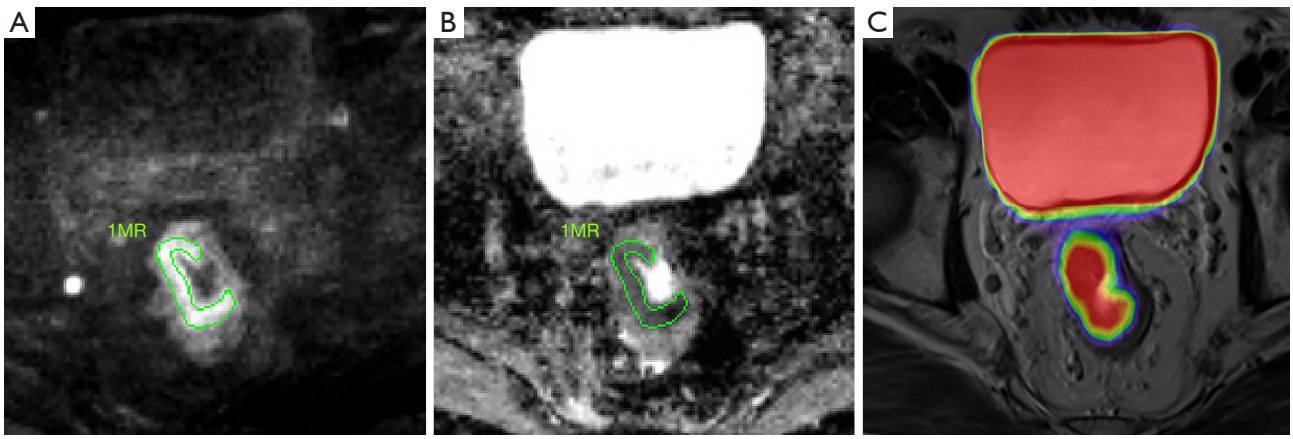

Figure 3 The b =800 s/mm^2 DWI (A), ADC map (B), and fused axial T2-weighted and ^{18}F-FDG PET image (C), all acquired by hybrid PET/MR. The ADC value was measured by drawing the ROI along the edge of the largest section of tumor area on the DWI image with a b-value of 800 s/mm^2, and the ROIs were copied to the corresponding ADC map to calculate the ADCmean and ADCmin. ADC, apparent diffusion coefficient; DWI, diffusion-weighted imaging; ^{18}F-FDG PET, fluorine-18-fluorodeoxyglucose-positron emission tomography; MR, magnetic resonance; ROI, region of interest.

ADC (ADCmean) and minimum ADC (ADCmin) were automatically measured (using a single slide measurement). We usually referred to the ADC value as the ADCmean value.

Histopathologic evaluation

After surgery, the histopathological examination of resected specimens was performed by expert colorectal pathologists according to the American Joint Committee on Cancer (AJCC) TNM staging system (21), which incorporates tumor status, lymph node status, and status of present metastases. The expressions of molecular markers, including epidermal growth factor receptor (EGFR), post-meiotic segregation increased 2 (PMS2), mut L homologue 1 (MLH1), human epidermal growth factor receptor 2 (HER2), Ki-67, mut S homologue 6 (MSH6), and mut S homologue 2 (MSH2), were also analyzed. The molecular markers were routinely examined by the Department of Pathology. Surgical specimens were stained with hematoxylin and eosin (HE) according to standard histologic protocol.

Two pathologists (JHL and WJ, with 5 and 10 years of experience, respectively) who were blinded to the results of the image analysis evaluated the TSR and dominant stromal cell type. The pathologists scored the TSR together, and they resolved any disagreement through discussion. The TSR was quantified as previously described (8). The largest

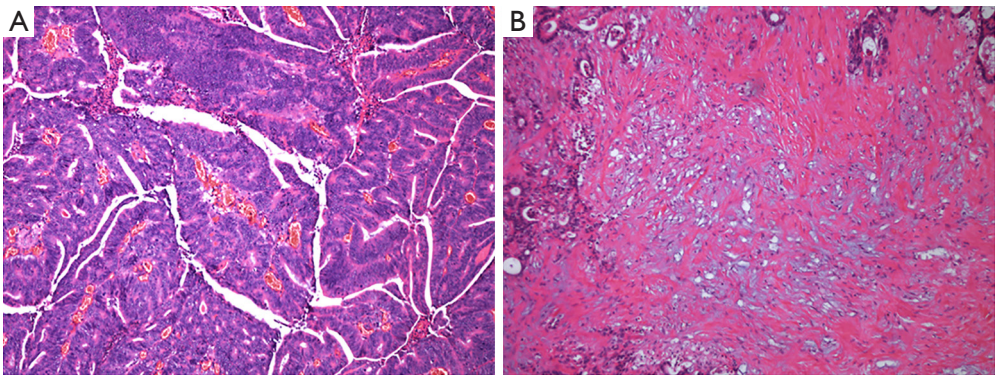

Figure 4 HE-stained sections of rectal cancer at ×100 magnification. (A) Section with TSR estimated as 90% (stroma poor). (B) Section with TSR estimated as 10% (stroma rich). HE, hematoxylin and eosin; TSR, tumor-stroma ratio.

invasive tumor was identified using a ×4 objective. Then, using a ×10 objective, an area was selected where both tumor and stromal tissue were present and tumor cells were visible on all slides of the image field. The TSR was defined as TSR = 100% (intratumoral tumor area)/(tumor area + intratumoral stroma area), and was scored using 10% increments (e.g., 10%, 20%, 30%). The tumors were defined as stroma high (50% TSR) and stroma low (>50% TSR), as suggested in previous studies (*Figure 4*) (8,22). Three stromal components, fibroblast, lymphocyte, and collagen, were also evaluated, as previously suggested (8). The dominant cell type was defined as fibroblast if the stroma comprised randomly oriented, immature collagen in a myxoid background. The dominant cell type was defined as lymphocyte if the stroma was predominantly composed of lymphocytes. The dominant cell type was defined as collagen if the stroma comprised broad bands of eosinophilic, hyalinized collagen.

Statistical analysis

Statistical analyses were performed using the software SPSS 22.0 (IBM Corp., Armonk, NY, USA). All data distributions were evaluated using the Kolmogorov-Smirnov test to evaluate normality and the Levene's test to evaluate the homogeneity of variance. Continuous variables were presented as mean ± standard deviation (SD). Student's *t*-tests were used to compare the statistical difference of parameters between the stroma-rich and stroma-poor group of lesions in rectal cancer patients. To analyze parameters that did not conform to normality or show homogeneity of variance, non-parametric Mann-Whitney U tests were used to compare the statistical differences between the 2 patient groups. Chi-square tests were used to test the statistical differences of counting data. A receiver operating characteristic (ROC) curve analysis was also performed to determine whether the cut-off values for ADCmean could be used to differentiate between high and low TSRs in patients. Pearson's correlation or Spearman's rank correlation were used to evaluate the correlations between ADC values (ADCmean and ADCmin), PET-related parameters (SUVmean, SUVmax, MTV, and TLG), and pathological indices. Intra-observer and inter-observer agreements were assessed with intraclass correlation coefficients (ICCs). Mean imputation method was applied for missing data. A P value <0.05 was considered statistically significant.

Results

Patient characteristics

Between December 2016 and March 2019, 72 patients with pathologically confirmed primary rectal cancer were examined preoperatively with whole-body ^{18}F-FDG-PET/MRI. However, data from 6 patients had to be excluded: 1 patient died within 30 days after surgery, and the DWI data sets of 5 patients were of inferior quality, preventing quantitative analysis. Thus, the final study cohort comprised 66 patients (*Figure 1*). Based on the TSR, the rectal cancer patients were categorized as stroma-rich (proportion of males: 63.4%, mean age: 61.59±11.25 years; n=41) and stroma-poor (proportion of males: 60.0%, mean age: 56.36±9.08 years; n=25). The clinicopathologic findings of the 2 patient groups are presented in *Table 1*. There were no statistical differences in the clinicopathologic parameters

Table 1 Clinicopathologic findings of rectal cancer patients according to TSR

Clinicopathological characteristics	TSR		P value
	Stroma high (n=41)	Stroma low (n=25)	
Male gender, n (%)	26 (63.4)	15 (60.0)	0.781
Age (years)	61.59±11.25	56.36±9.08	0.054
TSR scores	69.51%±12.03%	26.00%±11.55%	
Dominant cell type			0.304
Fibroblast	38	20	
Lymphocyte	1	2	
Collagen	2	3	
LD (cm)	4.42±1.88	3.65±1.31	0.074
pT			0.110
T1	2	3	
T2	12	10	
T3	23	11	
T4	4	1	
pN			0.853
N0	26	16	
N1	10	4	
N2	5	5	
Differentiation grade			0.405
Poorly	7	4	
Moderately	33	18	
Well	1	3	

Data given as the mean ± SD. TSR, tumor-stroma ratio; LD, the largest diameter of the tumor; pT, pathological tumor stage; pN, pathological nodal stage; SD, standard deviation.

(including the largest diameter of the tumor, pathological tumor stage, pathological nodal stage, and differentiation grade) between the stroma-rich and stroma-poor groups.

TSR in rectal cancer

The ADC values and PET-related parameters according to TSR are summarized in *Table 2*. The ADCmean values were significantly lower in the stroma-high group than the stroma-low group [(813.54±88.68) *vs.* (879.92±133.18)×10^{-3} mm^2/s, P=0.018; *Figure 5A*]. The ROC analysis identified a cut-off value of 776.5×10^{-3} mm^2/s for the ADCmean for discriminating between the TSR of stroma-high patients and stroma-low patients (*Figure 5B*). The area under the ROC curve (AUC) was 0.629 [95% confidence interval (CI): 0.492–0.766], and the sensitivity and the specificity of the ADCmean used for the discrimination of the TSR in patients with high and low TSRs was 0.920 and 0.341, respectively. However, there were no statistical differences in the ADCmin, SUVmean, SUVmax, MTV, and TLG between the 2 groups of rectal cancer patients (all P>0.05).

Table 2 The ADC values and PET-related parameters according to TSR

Image parameters	TSR		P value
	Stroma high (n=41)	Stroma low (n=25)	
ADCmean (×10^{-3} mm^2/s)	813.54±88.68	879.92±133.18	0.018
ADCmin (×10^{-3} mm^2/s)	660.71±136.05	648.44±185.15	0.758
SUVmean	9.35±4.21	9.89±5.20	0.647
SUVmax	15.2±6.64	16.45±8.86	0.546
MTV	11.5±8.23	11.15±7.88	0.865
TLG	109.65±90.80	112.73±101.30	0.899

Data given as the mean ± SD. ADC, apparent diffusion coefficient; PET, positron emission tomography; TSR, tumor-stroma ratio; SUV, standard uptake value; MTV, metabolic tumor volume; TLG, total lesion glycolysis; SD, standard deviation.

Association between image parameters and clinicopathologic factors

The correlation between image parameters and clinicopathological indices are summarized in *Tables 3,4*. Our results showed that the ADCmean values correlated with the TSR (r=0.327, P=0.007; *Figure 5C*). We found that the ADCmean and ADCmin values negatively correlated with the pathological T stages (r=–0.384, P=0.001; r=–0.416, P=0.001, respectively) as well as the largest diameters of the tumor (r=–0.340, P=0.005; r=–0.314, P=0.010, respectively) in rectal cancer patients. In addition, we found that the pathological T stages correlated with all PET-related metabolic parameters, including SUVmean, SUVmax, MTV, and TLG (r=0.338, P=0.006; r=0.350, P=0.004; r=0.326, P=0.007; and r=0.472, P<0.001, respectively). However, the image parameters were not correlated with the pathological N stages, the differentiation grades, the

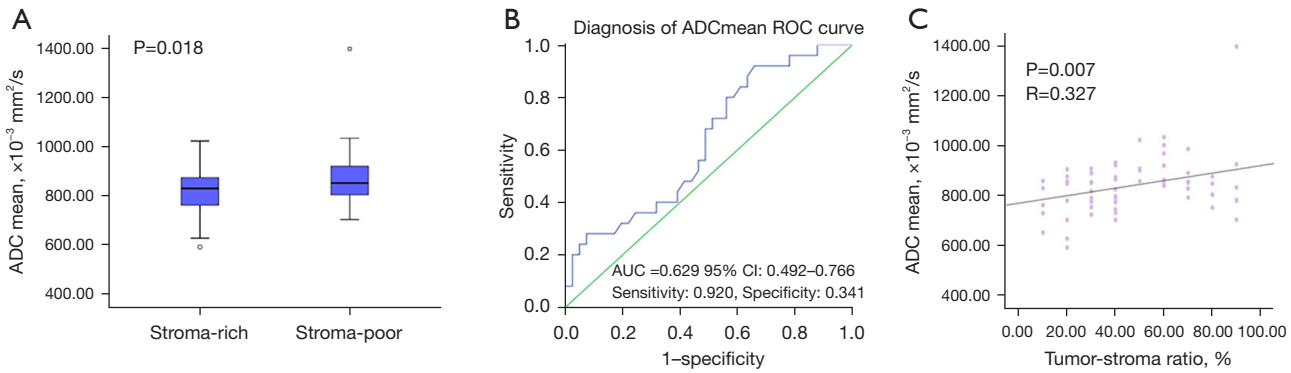

Figure 5 Quantitative analysis. Differences in ADCmean between stroma-rich patients and stroma-poor patients (A). ROC curve using the ADCmean (×10^{-3} mm^2/s) to differentiate the TSR (%) between stroma-rich patients and stroma-poor patients (B). Scatterplot showing correlation between ADCmean (×10^{-3} mm^2/s) and TSR (%) (C). ADC, apparent diffusion coefficient; ROC, receiver operating characteristic; AUC, area under the receiver operating characteristic curve; CI, confidence interval; TSR, tumor-stroma ratio.

dominant cell types, and all the molecular markers in rectal cancer patients (all P>0.05).

Association between ADC values and PET-related parameters

As shown in *Table 5*, the ADCmin values were correlated with SUVmean, SUVmax, and TLG (r=–0.335, P=0.006; r=–0.343, P=0.005; and r=–0.343, P=0.005, respectively; *Figure 6*) in rectal cancer patients. However, the ADCmean values were not correlated with any PET-related parameters, including the SUVmean, SUVmax, MTV, and TLG (all P>0.05).

Inter- and intra-observer variability

Table 6 summarizes the inter- and intra-observer variability for the ADC and PET analyses. As shown, the ICCs for intra- and inter-observer variability of the ADCmean values were 0.873 and 0.792; the ICCs for intra- and inter-observer variability of the ADCmin values were 0.911 and 0.935. Furthermore, the ICCs for the intra- and inter-observer variability of PET-related parameters were (0.996–1.000) and (0.999–1.000), respectively. The inter- and intra-observer agreements were considered excellent for all parameters.

Discussion

Emerging evidence indicates that tumor progression is a disease involving complex interactions within cancer tissue, and previous research has addressed the tumor microenvironment with regard to the stimulation of tumor progression and invasion (7). The tumor microenvironment is heterogeneous and composed of tumor cells and surrounding stroma, with the tumor stroma mainly composed of immune cells, fibroblasts, vascular endothelial cells, and extracellular matrix (7). Fibroblast is the major cellular component of stroma and plays an important role in tumor-stroma interactions which contribute to tumor progression and expansion (23). Several studies have evaluated the TSR in relation to the microenvironment of cancer, some of which have reported that the TSR is an independent prognostic factor in rectal cancer, and a greater proportion of stroma is associated with poorer patient outcomes (11,24).

Several studies have concluded that a lower ADC might be manifested as more aggressive biologic behavior in rectal cancer (25,26). A recent study found that the ADCmean positively correlated with the TSR in patients with rectal cancer (27). However, another study indicated that there were no statistical differences in the ADCmin or ADCmean between the stroma-poor and stroma-rich patients with rectal cancer, and the ADC values did not correlate with the TSR (28). Our results showed that the ADCmean values correlated with the TSR, and patients with stroma-rich rectal cancer had relatively lower ADCmean values. This result supports the hypothesis that the TSR influences the invasive behavior of rectal cancer. We assume that stroma-rich tumors produce more fibrotic, collagen-rich stroma, and the distribution of collagen increases interstitial fluid pressure and osmotic pressure, which inhibits water

Table 3 Correlations between the image parameters and clinicopathologic findings

Parameters	TSR		Dominant cell type		LD		T stage		N stage		Differentiation grade	
	r (95% CI)	P	r (95% CI)	P	r (95% CI)	P	r (95% CI)	P	r (95% CI)	P	r (95% CI)	P
ADCmean	0.327 (0.084, 0.513)	0.007	−0.181 (−0.414, 0.113)	0.145	−0.340 (−0.539, −0.097)	0.005	−0.384 (−0.576, −0.141)	0.001	0.048 (−0.204, 0.288)	0.703	0.129 (−0.131, 0.359)	0.302
ADCmin	0.020 (−0.266, 0.276)	0.871	−0.065 (−0.361, 0.246)	0.604	−0.314 (−0.497, −0.059)	0.010	−0.416 (−0.624, −0.185)	0.001	0.057 (−0.225, 0.248)	0.650	0.072 (−0.144, 0.278)	0.563
SUVmean	−0.058 (−0.330, 0.211)	0.641	−0.133 (−0.376, 0.128)	0.287	0.200 (−0.006, 0.397)	0.107	0.338 (0.075, 0.569)	0.006	0.036 (−0.203, 0.285)	0.774	−0.141 (−0.413, 0.142)	0.259
SUVmax	−0.027 (−0.319, 0.246)	0.829	−0.133 (−0.378, 0.129)	0.287	0.212 (0.013, 0.402)	0.088	0.350 (0.090, 0.578)	0.004	0.053 (−0.188, 0.297)	0.675	−0.157 (−0.428, 0.125)	0.209
MTV	−0.101 (−0.342, 0.160)	0.419	−0.076 (−0.358, 0.215)	0.545	0.783 (0.641, 0.876)	<0.001	0.326 (0.069, 0.535)	0.007	0.105 (−0.146, 0.362)	0.402	0.135 (−0.102, 0.389)	0.281
TLG	−0.100 (−0.385, 0.184)	0.425	−0.158 (−0.386, 0.126)	0.207	0.745 (0.618, 0.851)	<0.001	0.472 (0.232, 0.675)	<0.001	0.103 (−0.151, 0.357)	0.409	0.019 (−0.241, 0.286)	0.881

TSR, tumor-stroma ratio; LD, the largest diameter of the tumor; CI, confidence interval; ADC, apparent diffusion coefficient; SUV, standard uptake value; MTV, metabolic tumor volume; TLG, total lesion glycolysis.

Table 4 Correlations between the image parameters and molecular markers

Parameters	EGFR		PMS2		MLH1		HER2		Ki-67		MSH6		MSH2	
	r (95% CI)	P	r (95% CI)	P	r (95% CI)	P	r (95% CI)	P	r (95% CI)	P	r (95% CI)	P	r (95% CI)	P
ADCmean	−0.056 (−0.291, 0.156)	0.663	−0.053 (−0.300, 0.219)	0.683	0.055 (−0.233, 0.326)	0.669	−0.128 (−0.376, 0.137)	0.317	−0.049 (−0.261, 0.198)	0.699	−0.061 (−0.283, 0.237)	0.640	−0.082 (−0.306, 0.165)	0.526
ADCmin	−0.062 (−0.340, 0.204)	0.628	−0.141 (−0.383, 0.101)	0.272	−0.069 (−0.330, 0.194)	0.593	−0.079 (−0.347, 0.199)	0.536	−0.031 (−0.297, 0.237)	0.806	−0.008 (−0.209, 0.238)	0.948	−0.065 (−0.284, 0.164)	0.614
SUVmean	0.102 (−0.180, 0.352)	0.425	−0.070 (−0.296, 0.153)	0.588	−0.146 (−0.394, 0.104)	0.255	0.092 (−0.169, 0.336)	0.474	−0.191 (−0.455, 0.080)	0.128	−0.047 (−0.329, 0.231)	0.717	−0.177 (−0.434, 0.109)	0.170
SUVmax	0.087 (−0.211, 0.351)	0.495	−0.083 (−0.305, 0.131)	0.519	−0.167 (−0.411, 0.088)	0.190	0.081 (−0.173, 0.334)	0.527	−0.186 (−0.440, 0.087)	0.137	−0.046 (−0.326, 0.229)	0.721	−0.194 (−0.439, 0.090)	0.131
MTV	0.159 (−0.155, 0.416)	0.211	0.028 (−0.225, 0.266)	0.830	−0.078 (−0.310, 0.182)	0.541	0.125 (−0.140, 0.385)	0.329	0.096 (−0.169, 0.317)	0.445	−0.021 (−0.274, 0.227)	0.868	−0.119 (−0.398, 0.178)	0.356
TLG	0.112 (−0.145, 0.341)	0.379	−0.032 (−0.258, 0.205)	0.802	−0.142 (−0.366, 0.110)	0.268	0.080 (−0.197, 0.338)	0.531	0.061 (−0.151, 0.249)	0.628	−0.034 (−0.340, 0.231)	0.790	−0.144 (−0.420, 0.125)	0.265

EGFR, epidermal growth factor receptor; PMS2, post-meiotic segregation increased 2; MLH1, mut L homologue 1; HER2, human epidermal growth factor receptor 2; MSH6, mut S homologue 6; MSH2, mut S homologue 2; CI, confidence interval; ADC, apparent diffusion coefficient; SUV, standard uptake value; MTV, metabolic tumor volume; TLG, total lesion glycolysis.

Table 5 Correlations between the PET parameters and DWI parameters

PET parameters	ADCmean		ADCmin	
	r (95% CI)	P	r (95% CI)	P
SUVmean	−0.184 (−0.373, 0.078)	0.139	−0.335 (−0.52, −0.109)	0.006
SUVmax	−0.179 (−0.363, 0.079)	0.151	−0.343 (−0.530, −0.109)	0.005
MTV	−0.091 (−0.321, 0.084)	0.465	−0.153 (−0.341, 0.019)	0.219
TLG	−0.210 (−0.412, −0.022)	0.091	−0.343 (−0.496, −0.192)	0.005

PET, positron emission tomography; DWI, diffusion-weighted imaging; ADC, apparent diffusion coefficient; CI, confidence interval; SUV, standard uptake value; MTV, metabolic tumor volume; TLG, total lesion glycolysis.

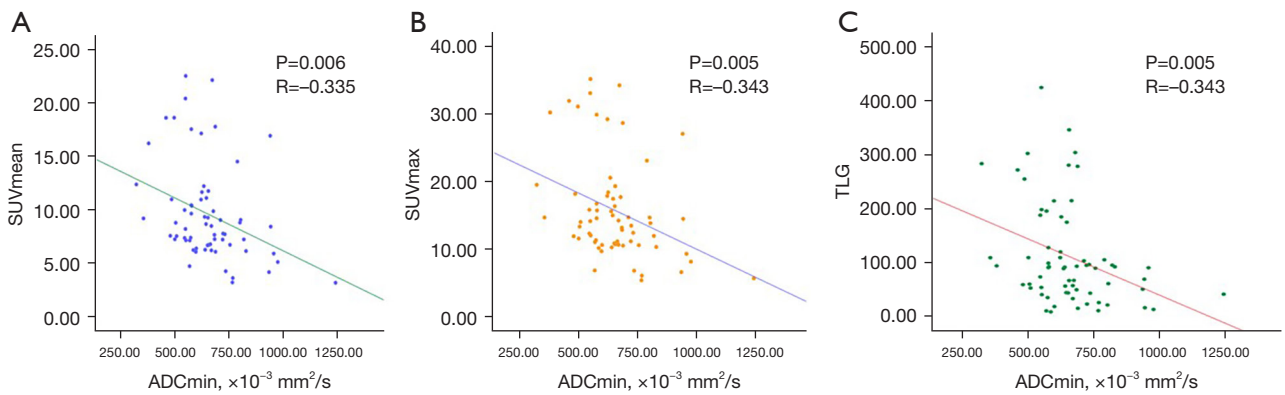

Figure 6 Scatterplots showing correlation between ADCmin (×10^{-3} mm^2/s) and SUVmean, SUVmax, and TLG. ADC, apparent diffusion coefficient; SUV, standard uptake value; TLG, total lesion glycolysis.

Table 6 Inter- and intra-observer variability of image parameters

Image parameters	Intra-observer (n=66)		Inter-observer (n=66)	
	ICC	95% CI	ICC	95% CI
ADCmean	0.873	(0.793, 0.922)	0.792	(0.609, 0.883)
ADCmin	0.935	(0.894, 0.960)	0.911	(0.855, 0.946)
SUVmean	0.999	(0.999, 1.000)	0.997	(0.995, 0.998)
SUVmax	1.000	(1.000, 1.000)	1.000	(1.000, 1.000)
MTV	0.999	(0.999, 1.000)	0.996	(0.993, 0.998)
TLG	1.000	(0.999, 1.000)	0.999	(0.998, 0.999)

All P<0.001. ICC, intraclass correlation coefficient; CI, confidence interval; ADC, apparent diffusion coefficient; SUV, standard uptake value; MTV, metabolic tumor volume; TLG, total lesion glycolysis.

diffusion and causes a subsequent decrease in the ADCmean values (29,30). The invasiveness of rectal cancer is considered a multifactorial process, and there is still no gold standard that is universally accepted. Therefore, we argue that the TSR can be applied clinically as a supplementary pathological diagnostic investigation to optimize risk stratification in the evaluation of rectal cancer.

The TNM staging system is still regarded the most important factor for estimating patient prognosis, and many studies have focused on the T staging of rectal cancer using

DWI (3). In our study, we found that the ADCmean and ADCmin values negatively correlated with the pathological T stages as well as the largest diameters of the tumor in rectal cancer. This result could be explained by the influence of cellular density and other histological components in the tumor tissue microenvironment on the ADC values (12,31). The higher T stage and larger tumor diameter may result in a tumor microenvironment with greater tumor cell density and other histological components. Accordingly, the reduction of the ADC values was likely the result of the more restricted diffusion movement of the water molecules. In addition, we found that the pathological T stages correlated with all PET-related metabolic parameters, including SUVmean, SUVmax, MTV, and TLG. This result suggests that tumors with lower ADC values and higher SUV values might exhibit more aggressive biologic behavior in rectal cancer.

Compared with microsatellite stability, microsatellite instability was less prone to metastasis (32). The expression of tumor tissue mismatch repair proteins, MLH1, MSH2, MSH6, and PMS2, could reflect microsatellite instability status. The Ki67 protein is a nuclear antigen, which can objectively reflect the state of tumor cell proliferation and indicate prognosis (33); EGFR is a transmembrane glycoprotein receptor which plays an important role in tumor occurrence and progression; moreover, anti-EGFR monoclonal antibody has been approved for a good response rate and possible secondary resection of advanced CRC (34). A previous study found that HER2 overexpression correlated with more aggressive CRC in a North African population (35). We found that the image parameters did not correlate with all the molecular markers in rectal cancer patients, which may relate to the limited sample size of patients in this study.

The major advantage of PET/MRI is that the simultaneous acquisition of PET and MRI data can minimize the misregistration artifacts and biologic changes. The SUVmax is the most commonly used and the most reproducible parameter for estimating the metabolic activity of FDG uptake. The SUVmean represents the average of the intensity of uptake, while TLG reflects both tumor metabolic activity and metabolic volume, which can reflect the cellular proliferation of the tumor. A study by Jeong *et al.* (36) reported that the ADCmean values of hybrid PET/MR showed a significant negative correlation with the SUVmax and SUVmean assessed by PET/computed tomography. Our results showed no correlation between the ADCmean values with SUVmax or SUVmean, but identified associations between the ADCmin values with SUVmean, SUVmax, and TLG, which is consistent with previously reported results (37). This can be explained by the fact that the ADCmin value has been considered to reflect the most proliferative portion and the highest tumor cell density of the tumor (38). We interpreted that the correlation between SUVmax and ADCmin probably represents the biologic relation between the metabolic activity and tumor cellularity, indicating that these two categories of parameters can be applied to describe tumor characteristics and plan treatment in rectal cancer.

To our knowledge, there are very few published research studies evaluating rectal cancer patients using PET/MRI, and the relationship between TSR and metabolic and functional features using PET/MRI in rectal cancer has not been reported previously. However, there were several limitations to this study. First, the sample size of this study was relatively small, hence, the statistical power was limited. Further studies with larger sample sizes are required. The PET/MRI examination is expensive, which limited the number of patients that could be included in the study. Second, there is likely to have been selection bias in this study, as the patients included in this study were limited to those who had undergone surgery without preoperative chemotherapy or radiation therapy. Third, because only a few of the patients included in this study had a distant metastasis and the follow-up duration was too short to evaluate recurrence, metastasis, and mortality, we did not analyze the survival outcome or correlation with metastases. Instead, we will aim to accomplish this in our future research endeavors over a longer follow-up period.

Conclusions

This hybrid PET/MRI study demonstrated a negative correlation between the ADCmin values with SUVmean, SUVmax, and TLG in rectal cancer. Additionally, our results showed that the ADCmean values correlated with the TSR, indicating that the intratumoral heterogeneity measured by PET/MRI may reflect characteristics of the tumor microenvironment. A better understanding of how tumor heterogeneity influences imaging parameters might be helpful for predicting tumor aggressiveness and prognosis.

Acknowledgments

Funding: None.

Footnote

Reporting Checklist: The authors have completed the STROBE reporting checklist. Available at https://qims.amegroups.com/article/view/10.21037/qims-21-938/rc

Conflicts of Interest: All authors have completed the ICMJE uniform disclosure form (available at https://qims.amegroups.com/article/view/10.21037/qims-21-938/coif). The authors have no conflicts of interest to declare.

Ethical Statement: The authors are accountable for all aspects of the work in ensuring that questions related to the accuracy or integrity of any part of the work are appropriately investigated and resolved. The study was conducted in accordance with the Declaration of Helsinki (as revised in 2013). The study was approved by the Institutional Review Board of The First Medical Center of Chinese PLA General Hospital (No. S2017-083-01), and informed consent was provided by all the patients.

References

1. Siegel RL, Miller KD, Goding Sauer A, Fedewa SA, Butterly LF, Anderson JC, Cercek A, Smith RA, Jemal A. Colorectal cancer statistics, 2020. CA Cancer J Clin 2020;70:145-64.
2. Tanaka A, Uehara K, Aiba T, Ogura A, Mukai T, Yokoyama Y, Ebata T, Kodera Y, Nagino M. The role of surgery for locally recurrent and second recurrent rectal cancer with metastatic disease. Surg Oncol 2020;35:328-35.
3. Zlobec I, Lugli A. Prognostic and predictive factors in colorectal cancer. J Clin Pathol 2008;61:561-9.
4. Figueredo A, Coombes ME, Mukherjee S. Adjuvant therapy for completely resected stage II colon cancer. Cochrane Database Syst Rev 2008;(3):CD005390.
5. Schmoll HJ, Van Cutsem E, Stein A, Valentini V, Glimelius B, Haustermans K, et al. ESMO Consensus Guidelines for management of patients with colon and rectal cancer. A personalized approach to clinical decision making. Ann Oncol 2012;23:2479-516.
6. Yokota J. Tumor progression and metastasis. Carcinogenesis 2000;21:497-503.
7. Lorusso G, Rüegg C. The tumor microenvironment and its contribution to tumor evolution toward metastasis. Histochem Cell Biol 2008;130:1091-103.
8. Ko ES, Han BK, Kim RB, Cho EY, Ahn S, Nam SJ, Ko EY, Shin JH, Hahn SY. Apparent diffusion coefficient in estrogen receptor-positive invasive ductal breast carcinoma: correlations with tumor-stroma ratio. Radiology 2014;271:30-7.
9. de Kruijf EM, van Nes JG, van de Velde CJ, Putter H, Smit VT, Liefers GJ, Kuppen PJ, Tollenaar RA, Mesker WE. Tumor-stroma ratio in the primary tumor is a prognostic factor in early breast cancer patients, especially in triple-negative carcinoma patients. Breast Cancer Res Treat 2011;125:687-96.
10. Huijbers A, Tollenaar RA, v Pelt GW, Zeestraten EC, Dutton S, McConkey CC, Domingo E, Smit VT, Midgley R, Warren BF, Johnstone EC, Kerr DJ, Mesker WE. The proportion of tumor-stroma as a strong prognosticator for stage II and III colon cancer patients: validation in the VICTOR trial. Ann Oncol 2013;24:179-85.
11. Geessink OGF, Baidoshvili A, Klaase JM, Ehteshami Bejnordi B, Litjens GJS, van Pelt GW, Mesker WE, Nagtegaal ID, Ciompi F, van der Laak JAWM. Computer aided quantification of intratumoral stroma yields an independent prognosticator in rectal cancer. Cell Oncol (Dordr) 2019;42:331-41.
12. Charles-Edwards EM, deSouza NM. Diffusion-weighted magnetic resonance imaging and its application to cancer. Cancer Imaging 2006;6:135-43.
13. Zhu Y, Zhou Y, Zhang W, Xue L, Li Y, Jiang J, Zhong Y, Wang S, Jiang L. Value of quantitative dynamic contrast-enhanced and diffusion-weighted magnetic resonance imaging in predicting extramural venous invasion in locally advanced gastric cancer and prognostic significance. Quant Imaging Med Surg 2021;11:328-40.
14. Curvo-Semedo L, Lambregts DM, Maas M, Beets GL, Caseiro-Alves F, Beets-Tan RG. Diffusion-weighted MRI in rectal cancer: apparent diffusion coefficient as a potential noninvasive marker of tumor aggressiveness. J Magn Reson Imaging 2012;35:1365-71.
15. Sun Y, Tong T, Cai S, Bi R, Xin C, Gu Y. Apparent Diffusion Coefficient (ADC) value: a potential imaging biomarker that reflects the biological features of rectal

cancer. PloS One 2014;9:e109371.
16. Sachs S, Bilfinger TV, Komaroff E, Franceschi D. Increased standardized uptake value in the primary lesion predicts nodal or distant metastases at presentation in lung cancer. Clin Lung Cancer 2005;6:310-3.
17. Berghmans T, Dusart M, Paesmans M, Hossein-Foucher C, Buvat I, Castaigne C, Scherpereel A, Mascaux C, Moreau M, Roelandts M, Alard S, Meert AP, Patz EF Jr, Lafitte JJ, Sculier JP; European Lung Cancer Working Party for the IASLC Lung Cancer Staging Project. Primary tumor standardized uptake value (SUVmax) measured on fluorodeoxyglucose positron emission tomography (FDG-PET) is of prognostic value for survival in non-small cell lung cancer (NSCLC): a systematic review and meta-analysis (MA) by the European Lung Cancer Working Party for the IASLC Lung Cancer Staging Project. J Thorac Oncol 2008;3:6-12.
18. Li TC, Wang LL, Liu BL, Hong JJ, Xu NN, Tang K, Zheng XW. Association between bone marrow fluorodeoxyglucose uptake and recurrence after curative surgical resection in patients with T1-2N0M0 lung adenocarcinoma: a retrospective cohort study. Quant Imaging Med Surg 2020;10:2285-96.
19. Schurink NW, Min LA, Berbee M, van Elmpt W, van Griethuysen JJM, Bakers FCH, Roberti S, van Kranen SR, Lahaye MJ, Maas M, Beets GL, Beets-Tan RGH, Lambregts DMJ. Value of combined multiparametric MRI and FDG-PET/CT to identify well-responding rectal cancer patients before the start of neoadjuvant chemoradiation. Eur Radiol 2020;30:2945-54.
20. Fernando S, Lin M, Pham TT, Chong S, Ip E, Wong K, Chua W, Ng W, Lin P, Lim S. Prognostic utility of serial 18F-FDG-PET/CT in patients with locally advanced rectal cancer who underwent tri-modality treatment. Br J Radiol 2020;93:20190455.
21. Amin MB, Greene FL, Edge SB, Compton CC, Gershenwald JE, Brookland RK, Meyer L, Gress DM, Byrd DR, Winchester DP. The Eighth Edition AJCC Cancer Staging Manual: Continuing to build a bridge from a population-based to a more "personalized" approach to cancer staging. CA Cancer J Clin 2017;67:93-9.
22. Mesker WE, Junggeburt JM, Szuhai K, de Heer P, Morreau H, Tanke HJ, Tollenaar RA. The carcinoma-stromal ratio of colon carcinoma is an independent factor for survival compared to lymph node status and tumor stage. Cell Oncol 2007;29:387-98.
23. Kalluri R, Zeisberg M. Fibroblasts in cancer. Nat Rev Cancer 2006;6:392-401.
24. Scheer R, Baidoshvili A, Zoidze S, Elferink MAG, Berkel AEM, Klaase JM, van Diest PJ. Tumor-stroma ratio as prognostic factor for survival in rectal adenocarcinoma: A retrospective cohort study. World J Gastrointest Oncol 2017;9:466-74.
25. Grosu S, Schäfer AO, Baumann T, Manegold P, Langer M, Gerstmair A. Differentiating locally recurrent rectal cancer from scar tissue: Value of diffusion-weighted MRI. Eur J Radiol 2016;85:1265-70.
26. Moon SJ, Cho SH, Kim GC, Kim WH, Kim HJ, Shin KM, Lee SM, Park JS, Choi GS, Kim SH. Complementary value of pre-treatment apparent diffusion coefficient in rectal cancer for predicting tumor recurrence. Abdom Radiol (NY) 2016;41:1237-44.
27. Cai C, Hu T, Gong J, Huang D, Liu F, Fu C, Tong T. Multiparametric MRI-based radiomics signature for preoperative estimation of tumor-stroma ratio in rectal cancer. Eur Radiol 2021;31:3326-35.
28. Zunder SM, Perez-Lopez R, de Kok BM, Raciti MV, van Pelt GW, Dienstmann R, Garcia-Ruiz A, Meijer CA, Gelderblom H, Tollenaar RA, Nuciforo P, Wasser MN, Mesker WE. Correlation of the tumour-stroma ratio with diffusion weighted MRI in rectal cancer. Eur J Radiol 2020;133:109345.
29. Liotta LA, Kohn EC. The microenvironment of the tumour-host interface. Nature 2001;411:375-9.
30. Heldin CH, Rubin K, Pietras K, Ostman A. High interstitial fluid pressure – an obstacle in cancer therapy. Nat Rev Cancer 2004;4:806-13.
31. Anderson AW, Xie J, Pizzonia J, Bronen RA, Spencer DD, Gore JC. Effects of cell volume fraction changes on apparent diffusion in human cells. Magn Reson Imaging 2000;18:689-95.
32. Kang S, Na Y, Joung SY, Lee SI, Oh SC, Min BW. The significance of microsatellite instability in colorectal cancer after controlling for clinicopathological factors. Medicine (Baltimore) 2018;97:e0019.
33. Klose J, Schmitt A, Pernthaler J, Warschkow R, Büchler MW, Schneider M, Lasitschka F, Tarantino I. Still proliferating CD44+/Ki67+ tumor cells after neoadjuvant radiochemotherapy identify rectal cancer patients with poor survival. Eur J Surg Oncol 2021;47:2078-86.
34. Suthar PP, Singh JS, Gupta K. 18F-FDG PET/CT Imaging Features of Cardiac Arrhythmia in a Patient Treated with Panitumumab. J Nucl Med Technol 2021;49:360-1.
35. Abdul Razzaq EA, Venkatachalam T, Bajbouj K, Rahmani M, Mahdami A, Rawat S, Mansuri N, Alhashemi H,

Hamoudi RA, Bendardaf R. HER2 overexpression is a putative diagnostic and prognostic biomarker for late-stage colorectal cancer in North African patients. Libyan J Med 2021;16:1955462.
36. Jeong JH, Cho IH, Chun KA, Kong EJ, Kwon SD, Kim JH. Correlation Between Apparent Diffusion Coefficients and Standardized Uptake Values in Hybrid (18)F-FDG PET/MR: Preliminary Results in Rectal Cancer. Nucl Med Mol Imaging 2016;50:150-6.
37. Er HÇ, Erden A, Küçük NÖ, Geçim E. Correlation of minimum apparent diffusion coefficient with maximum standardized uptake on fluorodeoxyglucose PET-CT in patients with rectal adenocarcinoma. Diagn Interv Radiol 2014;20:105-9.
38. Lee EJ, terBrugge K, Mikulis D, Choi DS, Bae JM, Lee SK, Moon SY. Diagnostic value of peritumoral minimum apparent diffusion coefficient for differentiation of glioblastoma multiforme from solitary metastatic lesions. AJR Am J Roentgenol 2011;196:71-6.

Cite this article as: Hu S, Xing X, Liu J, Liu X, Li J, Jin W, Li S, Yan Y, Teng D, Liu B, Wang Y, Xu B, Du X. Correlation between apparent diffusion coefficient and tumor-stroma ratio in hybrid ^{18}F-FDG PET/MRI: preliminary results of a rectal cancer cohort study. Quant Imaging Med Surg 2022;12(8):4213-4225. doi: 10.21037/qims-21-938

